Available online at www.sciencedirect.com

ScienceDirect

Procedia Manufacturing 16 (2018) 91–98

Procedia MANUFACTURING

www.elsevier.com/locate/procedia

7th International Conference on Through-life Engineering Services

Mechanical performance of composite bonded joints in the presence of localised process-induced zero-thickness defects

Hamed Yazdani Nezhad[a,*], Dimosthenis Stratakis[a], David Ayre[a], Sri Addepalli[b], Yifan Zhao[b]

[a]*Enhanced Composites & Structures Centre, School of Aerospace, Transport & Manufacturing, Cranfield University, United Kingdom*
[b]*Through-life Engineering Services Centre, School of Aerospace, Transport & Manufacturing, Cranfield University, United Kingdom*

Abstract

Processing parameters and environmental conditions can introduce variation into the performance of adhesively bonded joints. The effect of such variation on the mechanical performance of the joints is not well understood. Moreover, there is no validated non-destructive inspection (NDI) available to ensure bond integrity post-process and in-service so as to guarantee initial and continued airworthiness in aerospace sector. This research studies polymer bond defects produced in the laboratory scale single-lap composite-to-composite joints that may represent the process-induced defects occurring in actual processing scenarios such as composite joining and repair in composite aircrafts. The effect of such defects on the degradation of a joint's mechanical performance is then investigated via quasi-static testing in conjunction with NDI ultrasonic C-scanning and pulsed thermography. This research is divided into three main sections: 1- manufacturing carbon fibre-reinforced composite joints containing representative nearly zero-thickness bond defects, 2- mechanical testing of the composite joints, and 3- assessment of the NDI capability for detection of the bond defects in such joints.

© 2018 The Authors. Published by Elsevier B.V.
This is an open access article under the CC BY-NC-ND license (https://creativecommons.org/licenses/by-nc-nd/4.0/)
Peer-review under responsibility of the scientific committee of the 7th International Conference on Through-life Engineering Services.

Keywords: composite joint; adhesive bonding; airworthiness; bond degradation; non-destructive inspection; cohesive failure

* Corresponding author. Tel.: +44(0)1234750111.
E-mail address: h.yazdani-nezhad@cranfield.ac.uk

2351-9789 © 2018 The Authors. Published by Elsevier B.V.
This is an open access article under the CC BY-NC-ND license (https://creativecommons.org/licenses/by-nc-nd/4.0/)
Peer-review under responsibility of the scientific committee of the 7th International Conference on Through-life Engineering Services.
10.1016/j.promfg.2018.10.175

1. Introduction

Over the last decades, use of adhesively bonded joints have been increased in the assembly of aircrafts' primary structures e.g. fuselage and wing structures [1] with much less weight penalty compared to use of metallic fasteners. Use of bonding in composite structures is more advantageous than fasteners as it does not require drilling holes that cuts through reinforcements e.g. carbon fibres, since damage to continuous fibres can initiate premature failure in polymer composites. Fastener joints are also prone to large stress concentrations and damage around the fastening area [2-5]. Adhesive bonding can provide a smooth load transfer and reduced associated stress concentrations [6, 7].

Moreover, the mechanical strength, the corrosion resistance and durability of structural adhesives have been significantly improved. This has allowed the replacement of mechanically fastened joints with adhesively bonded ones [8] e.g. in composite aircraft [9] though adhesive joints in aircrafts' primary structures still require secondary mechanical fasteners to comply with aviation certifications e.g. FAA-AC20 [10]. More specifically, adhesives are used to bond the stringers to fuselage and wing skins to stiffen the structures against buckling [1]. To use adhesive joints in primary structures, it must be ensured that the bonds are effective and integrated with the composite adherends, and stay effective in-service [5]. Therefore a full understanding of the type of defects that may affect the joint performance must be established. Categories of zero-thickness bond defects are identified as the most challenging defects to detect non-destructively while their effect on the joint strength can become significant [6, 11]. Such defects can also be present in interlaminar bonds of composite laminates, and have numerically been found to dissipate more than 65% of the strain energy induced by dynamic events such as impact [12], also difficult to detect via NDI. In addition, unknown damage tolerance behaviour of bonded joints in size scaling is a major problem. The assessment of damage tolerance must ensure that where fatigue, intrinsic/discrete damage, manufacturing flaws, or severe accidental damage occurs within the operational life of aircraft [13], the remaining structure will sustain operational loads without failure or excessive deformation until the damage is detected [14-16]. Therefore, it is necessary for diagnostic tools to detect, characterise and categorise the composite damage. The aim of this research is to investigate damage behaviour of single-lap composite bonded joints in the presence of localised nearly zero-thickness defects, in aerospace grade joints manufactured in different geometries in order to address the size scaling issue.

2. Materials

2.1. Composite adherends: Carbon fibre-reinforced polymer (CFRP) composites were manufactured from unidirectional prepreg HexPly® 8552/268GSM/IM7 material. HexPly® 8552 is a high-performance toughened epoxy for use in primary aerospace structures. HexTow® IM7 is a continuous, intermediate modulus carbon fibre [17].

2.2. Adhesive: The adhesive material was the adhesive film Cytec® FM94 (0.25mm thickness), a modified epoxy adhesive tape designed for bonding metallic and composite structures. It offers high-temperature performance (service temperature: 104°C), toughness and moisture resistance. Moreover, FM94 exhibits superior elongation, toughness and shear strength properties. The controlled flow characteristics allow for its use in co-cured applications and bonding.

2.3. *Pre-treatment product:* Oxford Advanced Surfaces has provided Onto™ SB1050, a functional surface treatment, that improves the adhesive bond strength in bonded systems [18]. Such treatment, used in the current research, was designed to promote adhesion of polyurethane and epoxy adhesives, requiring no specialist coating equipment [19]. The pre-treatment was a chemical process. Two types of surface treatment were utilized: peel ply and the coupled Onto™ pre-treatment chemical. Peel ply is the most widely used, rapid and cost-effective technique for surface treatment since it ensures continue worthiness. However, it is not reliable for bonding as it cannot ensure good quality bond, compared to plasma treatment for instance. This is the reason that the Onto™ SB 1050 had been introduced. The coupled pre-treatment Onto™ SB 1050 chemical product was applied just before the adhesive bonding.

3. Manufacturing

3.1. Joint manufacturing

Joint specimens were manufactured with two different widths (25mm and 50mm) and different defect types, totalling four configurations. Specimens were identified as Category 0, I, II and III. Category 0 was the baseline, followed the bonded joining specifications, with no defect and a width of 50mm. No-defect specimens with 25mm width were not made as their data are now available in the authors' former research [6]. Category I contained a pre-

existing adhesion defect with the length of 5mm embedded throughout the width of the standard (25mm wide) joint. Category II and Category III had the same width of 50mm, and incorporate a 'thumb nail' shaped defect. The difference between these categories was that Category II used one layer of adhesive, while Category III used two layers as shown in Figure 1 to imitate adhesion failure (pre-existing damage between the adhesive and the composite adherend) and cohesion failure (pre-existing damage between two adhesive layers) respectively. Category I specimens adopted a width of 25mm and the type of the embedded defect was through-the-width, as illustrated in Figure 2.

The ASTM standard used was D3165 suggesting specimen geometry of 114mm (length)×25mm (width). However, the study also focused on wider specimens with 50mm width. The overlap length for all types was 25mm.

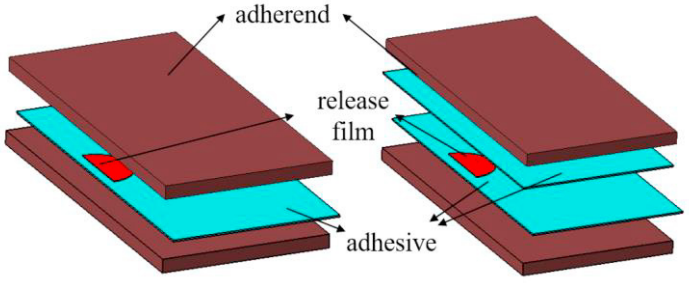


Figure 1: Schematic of defect Category II (a) and III (b)

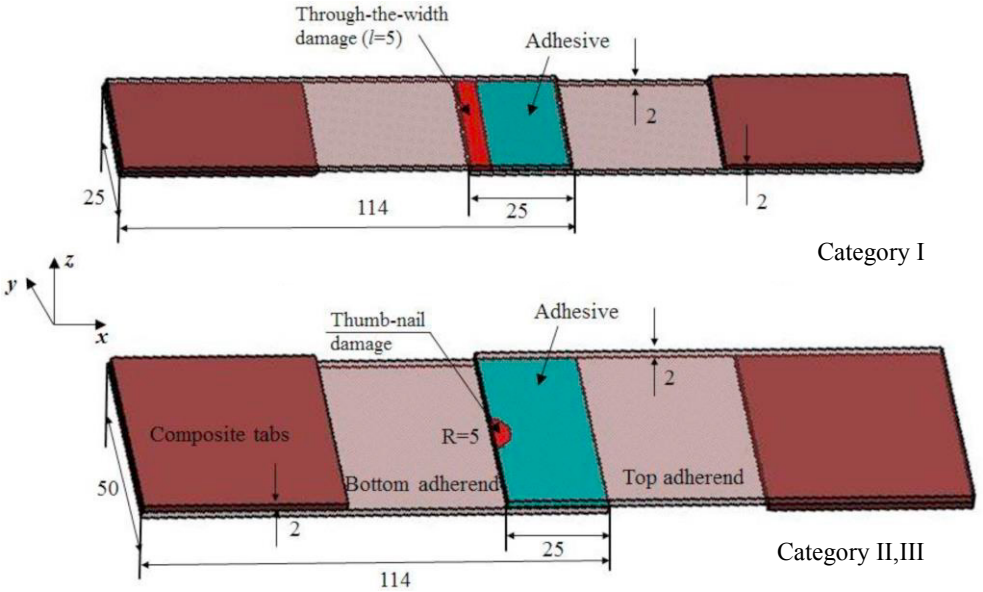


Figure 2: Schematic of narrow and wide joint specimens (all dimensions given in mm)

Composite adherends were manufactured using the HexPly® 8552/268GSM/IM7, via manual lay-up of pre-preg followed by autoclave curing according to the data sheet of HexPly® 8552. The dimensions of the composite panels produced were 600mm×600mm. To achieve uniform properties in all directions a quasi-isotropic lay-up was chosen. The laminate sequence was $[0/+45/90/-45]_S$. The thickness of each ply was 0.25mm and 8 plies were used in order to manufacture the panels. Therefore, the total thickness of such adherends was 0.25mm×8=2mm (nominal). The role of the surface quality is highly important during the bonding process because it is a crucial factor in order to ensure the quality of the adhesive bonding and therefore adhesion properties [20, 21]. For this research, a coupled surface treatment was utilised; peel ply followed by pre-treatment product of Advanced Oxford Surfaces Onto™ SB1050.

In general, peel ply is the most widely used technique for surface treatment since it ensures consistent results, is rapid and cost-effective [9, 11, 22, 23]. Peel ply cannot ensure a good quality bond [24] compared to plasma treatment.

This is the reason that the Onto™ SB1050 had been introduced just before the adhesive application: firstly, peel ply was removed, and then Onto™ was applied on the adherend surfaces just before assembling the adherends and adhesive in the uniformly pressurizing fixture preparing for curing inside a conventional heating oven.

3.2. Defect embedment

The embedment of the defects was carried out using the highly thin (nearly zero-thickness) semi-circular (thumb nail) release films with thickness of < 15 microns. It was applied before bonding, and removed post-curing.

The laboratory simulation of kissing bond defects has been chosen based on the author's previous research published in [6, 11]. In those researches, the mechanical response of the joints (failure load, displacement and failure mechanisms via fractography) in the presence of kissing bonds was studied. The defects were fabricated via two methods of release film embedment and pre-curing process in which no additional material/film was used, i.e. the adhesive and adherend surfaces were in contact but with no interaction. To do so, the adhesive at the central region (20mm × 20mm) of the bond overlap (25mm × 25mm) was fully cured on the surface of one adherend; the surrounding adhesive was embedded and fully cured to create interaction with the two adherends out of the central region. The testing data obtained from the two defect embedment methods showed identical mechanical response. Therefore, release film embedment technique was used for simplicity in the current article. However, note that such release films are not true representation of zero-thickness defects as any thickness associated with the films would result in less-conservative results compared to actual zero-thickness defects so the simulated damage would require more strain energy to propagate. However, such representation can reliably be used for the comparative studies presented herein.

The first stage was the creation of the two different types of defect. For the semi-circular defects in categories II and III, the radius was 5mm. The width of the through-the-width defect in category I was 5mm and the length was bigger than the length of the coupons (i.e. >25mm), in order to simplify the embedment. Very slight movement of the release films was observed post manufacturing, and thus its effect on our analysis was neglected.

3.3. Adhesive bonding

The bonded length of the joints was 25mm. Therefore the overlap area was 25mm×25mm (Category I Specimens) and 25mm×50mm for other specimens (0, II, III). The adhesive film FM94 was cut to the required size and fixed to one adherend. The backing paper of the film was removed before assembly with adherend as seen in Figure 3.

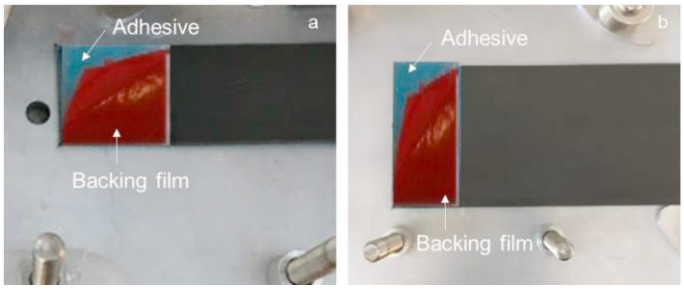


Figure 3: The removal of the backing film, a) narrow adherend, and b) wide adherend

The pre-treatment product Onto™ SB1050 was applied just before bonding. The bonding process was carried out by using a bonding fixture to give accurate bond length, proper alignment and uniform bond line thickness to the all single-lap joints. The required pressure (0.28MPa according to Specifications) was applied based on the required force for six specimens, which was the maximum number for this particular fixture. The force was maintained by using heavy plates on the bonded area fixed by compression springs, as illustrated in Figure 4. It is worth mentioning that for alignment of the joints, two alignment tabs (25mm×25mm and 25mm×50mm) were placed at the end of the joints, one beneath and one above. The reason was to balance the lap joint geometry in the fixture.

The fixture-joint assembly was initially pre-heated to 40°C in order to ensure that there was no lag in temperature between the jig and the oven. Moreover, for better monitoring of the curing process a thermocouple was attached on the plate. The oven was set to have a temperature rate of 1°C/min until it reached 121°C (max. temperature). The entire assembly temperature was held for one hour at 121°C, and then was cooled to 60°C prior to removal.

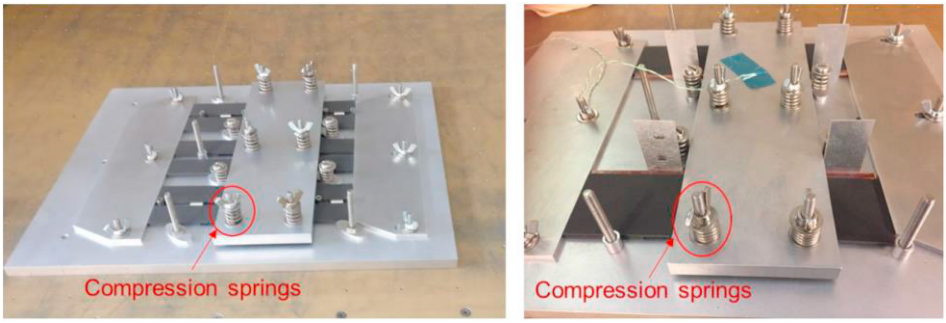


Figure 4: Pressure application with the compression springs

4. Single-lap shear testing

The lap shear tension testing of the bonded joints was carried out on an INSTRON 5500*R* testing machine. The experiment was carried out in order to determine the ultimate failure load and displacement of the joints (note that the stress-strain values are highly non-uniform across the bond length (herein 25mm for all joints) and thus the failure load and displacement levels have been studied instead [6, 11]). The specimens were mounted in self-tightening jaws. The test frame was fitted with a 100kN load cell, and testing was carried out using a rate of 1mm/min in a temperature controlled room, 21°C (±2°C). A laser extensometer used to measure displacement in the bonded overlap of the joints.

5. Non-destructive inspection

Sonatest ultrasonic C-scan equipment was used to investigate the positioning state of the embedded defects post-process. The setup of this machine consisted of an immersion tank with water and a pulse-echo transducer. The scanning speed was set at 30mm/s, the gain was 20dB and the frequency of the transducer was 5MHz.

In the presence of a defect, the strength of the reflected signal was reduced. The results from the test equipment provide a visual interpretation of the signal strength, where a colour palette associates signal strength to colour.
Also, the adhesively bonded joints were subjected to a high-energy pulsed light by implementing the Thermoscope II system of Imaging Inc. The pulsed thermography systems used two capacitor bank controlled xenon flash lamps and a 640x512 pixel, cooled FLIR SC 7600 MB infrared camera to complete the inspection. The data was captured at a frame rate of 50Hz for a total of 770 frames which included 10 pre-flash frames using the in-house Mosaiq software.

For the thermography test, the joints were mounted in a sealed black box (to reduce reflections due to external sources) and positioned 270mm in front of the camera's lens. Optical microscopy was also carried out subsequent to destructive testing to complement the NDI data, to visualise the defects and failure mechanisms.

6. Results and discussion

6.1. Force-displacement data

The failure load for the four categories are presented in Figure 5, and the failure displacement in Figure 6. Figure 5 also includes the ultimate average shear stress levels (equaling the ultimate failure load divided by the effective bond area) at top of each category. For no-defect joints (Cat. 0), the ultimate failure load for wide joints was 20.7kN and for narrow joints (Cat. I) was 7.8kN. Failure loads for Categories II and III fall between these two levels. Therefore, the average shear stress was 13.66MPa and 15.36MPa respectively. It can be noticed that there was a big difference in the shear stress. This is attributed to the fact that there is a high stress gradient through the bond with stresses being high at the bond edges [11, 16] and low at the bond centre, and thus an average stress level cannot be representative of the bond strength. Also, the joints exhibited a 30% and 48% reduction from the shear stress, which is attributed to surface treatment. Surface treatment such as grit blasting and plasma treatment are more effective in creating better adhesion than that provided by peel ply. Better performance can be achieved by utilising these techniques [25]. Also, peel ply was not followed by mechanical ablation. According to the findings in [26], this is highly recommended for creating chemically active surfaces. Also, the secondary bending occurring in composite joints is significant for single-lap joints due to their asymmetric nature. This introduced mixed-mode failure.

Category 0 seemed to exhibit the highest failure load as expected for a wide joint with no defect. This category had the most scattered data attributed to the introduction of higher out-of-plane mechanical fluctuations associated with

wide joints during tension testing. Category III (cohesion defect initiator) had a higher failure load than Category II (adhesion defect initiator), which was expected. This was because a joint with cohesive failure should fail at higher load as the failure is progressive in cohesion. In adhesion failure, the joint fails instantaneously (i.e. less progressive) and then lower load is reached. Category I (narrow joints) exhibited the lowest failure load because these specimens had smaller width (25mm). There is difference in failure response between the thumb-nail and through-the-width (Cat. I) defects. Thus, additional investigation is required in order to understand, better, the impact of these defects on the performance of the joints. Also, the failure displacement for Category 0 (no-defect) was found surprisingly lower than that in joints with defects (Figure 6). This can be attributed to the introduction of deformation mechanisms to the joints with defects where strain energy could have been dissipated more gradually around defects e.g. for blunting. This will be discussed further in section 6.2 where microscopy images from the damage sites are presented.

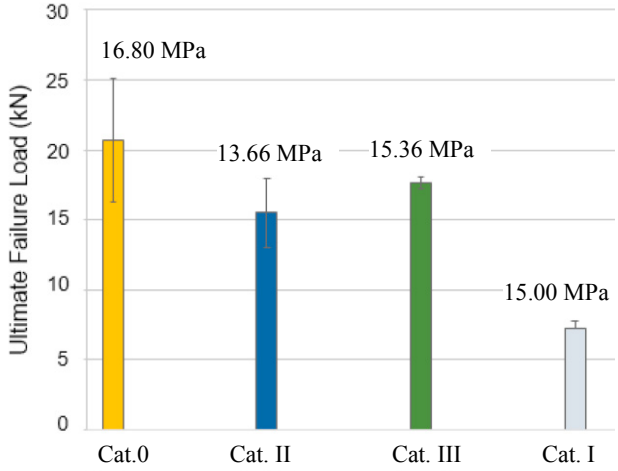


Figure 5: Ultimate failure loads for the bonded categories

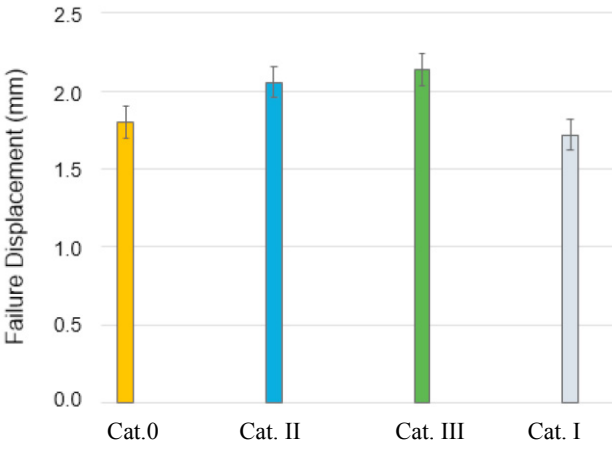


Figure 6: Failure displacements for the bond categories

6.2. Failure mechanisms and damage area

Figure 7 represents the ultrasonic C-scanning images. The signal changes (different in colour) at the centre of the width of specimens with the semi-circular defect and through-the-width defect. This clearly indicated a change in the material where the release film is present (pre-existing defect). C-scan successfully detected the embedded defects even through its small thickness (<15 microns). Moreover, there is an indication that the bond strength was not uniform in the overlap area as the contrast changes near the edge of the overlap (green colour). Overall, ultrasonic C-scan successfully detected the two types of defect. The results identified the location and the size of the defect. However, there is no established correlation between the strength of the bond and the received signal. Therefore, it is difficult to quantify the integrity and strength of the bond by utilising ultrasonic C-scan alone.

Figure 8 shows the pulsed thermography images. Thermography was able to detect the embedded defects however via less distinctive signal, in contrast to C-scanning. Thus, the identification of the defects was not clear. It was visualised from the microscopic images (not shown in the interests of space) that the adhesion failure was the failure mechanism for Category 0 (no pre-defect joints). The joints exhibited failure indicating that the adhesive had not bonded properly to the adherend - the adhesive peeled off completely. In addition, the adhesive acted like a brittle material. Moreover, these joints mainly exhibited interface delamination. This is attributed to deficiencies induced during the curing process and/or surface treatment. This may explain the difference in the failure load of the three joints (Figure 5). Category I joints also exhibited dominant adhesion failure, and brittle adhesive bulk failure.

Figure 9 shows the optical images for Category II. In this category, one layer of adhesive was applied in order to introduce pre-existing adhesion defects (between composite adherend and adhesive bond), thus introducing adhesion failure. The brittle behaviour of the adhesive can be observed. It can be seen that adhesion failure is the dominant failure mechanism. However, using the microscope, it can be observed that thin cohesion failure was also present.

Finally, Figure 10 shows the images for Category III. In this category, two layers of adhesive film were applied to introduce cohesion failure in-between; the release film was embedded between the two layers of adhesive to introduce

pre-existing cohesion defect (cohesive failure). The failure mode was mainly a mixed-mode failure (adhesion and cohesive failure initiated by cohesion failure). It was also observed that although delamination occurred in Cat. III, the integrity of the bond did not degrade as much, according to Figures 5 and 6.

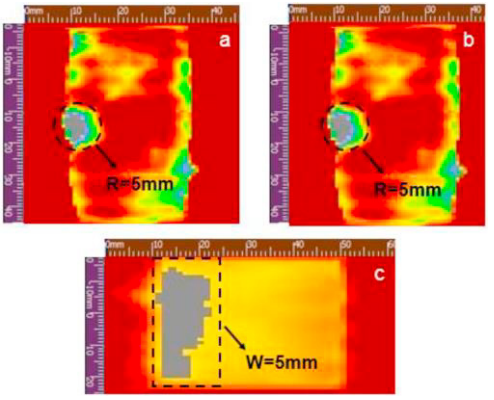


Figure 7: Ultrasonic images; (a) Cat. II, (b) Cat. III and (c) Cat. I

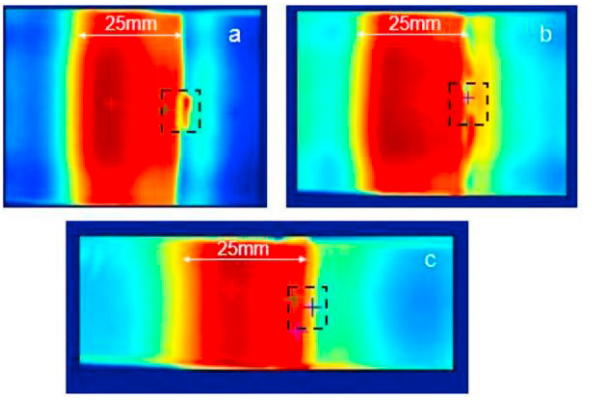
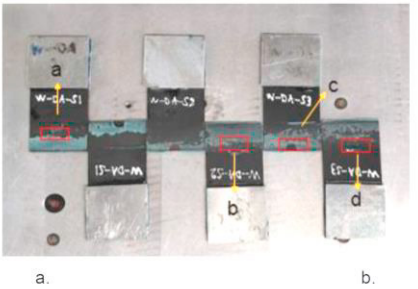


Figure 8: Pulsed thermography images; (a) Cat. II, (b) Cat. III and (c) Cat. I



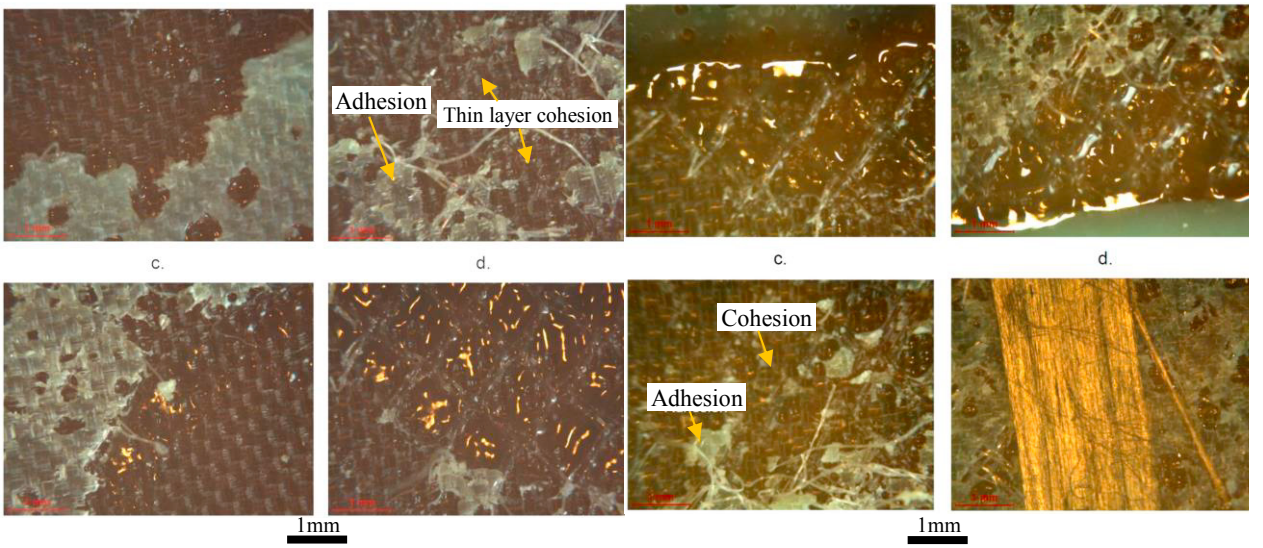


Figure 9: Cat. II joint failure surfaces (scale bar: 1mm)

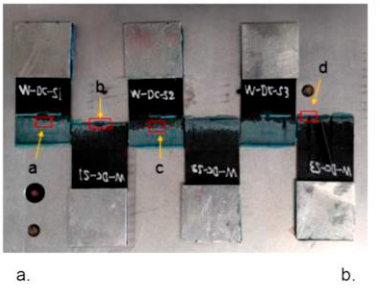


Figure 10: Cat. III joint failure surfaces (scale bar: 1mm)

7. Conclusions

The single-lap shear test indicated that there was a difference in the shear strength among the four categories of the localised defects introduced to the bond. Specifically, Category II exhibited 24.9% lower failure load compared to

Category 0 (standard 25mm-width joints), and Category III (50mm-width joints) exhibited 14.7% reduction in the ultimate failure load. However, considering the size scaling, defects such as those, i.e. localised within the joints, might affect the integrity of the whole structure; hence, their consideration in design of a bonded joint is quite important. According to the research in [6, 11], a kissing bond covering more than 65% of a bond area at the centre of a bond (ineffective region) may result in 30% reduction of the nominal strength in a conservative single-lap joint scenario. In addition, the two defect scenarios of Cat. II and III (single layer with pre-crack at the interface and doubled layer with pre-crack in the adhesive bulk, both thumb-nail shape defects) behaved identically in terms of failure load, failure displacement and failure mechanisms; hence, embedment of thin release film can be a representative of process-induced (e.g. curing), nearly zero-thickness bond defect for such single-lap joints either it's due to improper cure (bulk defect) or poor surface quality (interface defect), also evidenced in [6] for centrally located bond defects. The advantage with film embedment is that it enables NDI capability to detect such defects in laboratory examinations.

NDI was carried out to investigate the possibility of detecting the embedded defects. Ultrasonic C-Scanning showed more promising results compared to thermography. However, it was not possible to identify the integrity and degradation of the bond quality via direct correlation with the performance data (failure load and displacement). Lastly, cohesive failure was detected on the failed surfaces via microscopy. Although with a naked eye it seemed to be adhesion failure after damage initiation ahead of the pre-existing cohesion defect (Category III), it rapidly deviated towards the adhesive/adherend interface to ultimately and dominantly result in adhesion failure. However, it was not possible to correlate the failure mode with the defect types at this stage.

References

[1] Higgins, A., *Adhesive bonding of aircraft structures.* International Journal of Adhesion and Adhesives, 2000. **20**(5): p. 367-376.

[2] Yazdani Nezhad, H., et al., *Bearing damage characteristics of fibre-reinforced countersunk composite bolted joints subjected to quasi-static shear loading.* Composite Structures, 2017. **166**: p. 184-192.

[3] Zhou, Y.H., et al., *A study of intra-laminar damage in double-lap, multi-bolt, composite joints with variable clearance using continuum damage mechanics.* Composite Structures, 2014. **116**: p. 441-452.

[4] Zhou, Y.H., et al., *A three dimensional implicit finite element damage model and its application to single-lap multi-bolt composite joints with variable clearance.* Composite Structures, 2015. **131**: p. 1060-1072.

[5] Waugh, R.C., *Development of Infrared Techniques for Practical Defect Identification in Bonded Joints, PhD Research*. 2015: Springer.

[6] Bhanushali, R., D. Ayre, and H.Y. Nezhad, *Tensile Response of Adhesively Bonded Composite-to-composite Single-lap Joints in the Presence of Bond Deficiency.* Procedia CIRP, 2017. **59**: p. 139-143.

[7] Flom, Y. and R.J. Arsenault, *Interfacial bond strength in an aluminium alloy 6061 - SiC composite.* Mater. Sci. Eng., 1986. **77**: p. 191-197.

[8] Roach, D., R. Rackow, and R. Duvall, *Innovative Use of Adhesive Interface Characteristics to Nondestructively Quantify the Strength of Bonded Joints*, in *10th Eur. Conf. Non-Destructive Test.* 2010.

[9] Tracey, A.C., et al., *Improving Adhesive Bonding Through Surface Characterization : Reverse the Curse of the Nylon Peel Ply*. 2013, Boeing Co.

[10] Administration, F.A., *Advisory Circular AC20-107B: Composite Aircraft Structure*, U.S.D.o. Transportation, Editor. 2009.

[11] Nezhad, H.Y., et al., *A novel process - linked assembly failure model for adhesively bonded composite structures.* CIRP Annals- Manufacturing Technology, 2017: p. 5-5.

[12] Nezhad, H.Y., et al., *Numerical analysis of low-velocity rigid-body impact response of composite panels.* International Journal of Crashworthiness, 2015. **20**(1): p. 27-43.

[13] Soderquist, J.R., *Damage Tolerance Considerations in Composite Aircraft Structure*. 2016.

[14] Davis, M.J. and D.A. Bond, *Certification of Adhesive Bonds for Construction and Repair*, in *The Aging Aircraft Conference 2000*. 2000: St. Louis.

[15] Federal Aviation, A., *Composite Aircraft Structure*. 2009. p. 37-37.

[16] Baker, A., A.J. Gunnion, and J. Wang, *On the Certification of Bonded Repairs to Primary Composite Aircraft Components.* Journal of Adhesion, 2015. **91**(1-2): p. 4-38.

[17] *Product Data: HexTow ® IM7*. 2016. p. 1-3.

[18] Surfaces, O.A., *Onto TM SB1050 Onto TM SB1050 : Adhesion Promotion of Polyurethane and Epoxy Adhesives*.

[19] Surfaces, O.A., *Onto TM SB1050 Evaluation Pack Onto TM SB1050 Evaluation Pack Application Note*.

[20] Baldan, A., *Adhesively-bonded joints and repairs in metallic alloys, polymers and composite materials: Adhesives, adhesion theories and surface pretreatment.* Journal of Materials Science, 2004. **39**(1): p. 1-49.

[21] Baldan, A., *Adhesively-bonded joints in metallic alloys, polymers and composite materials: Mechanical and environmental durability performance.* Journal of Materials Science, 2004. **39**(15): p. 4729-4797.

[22] Benard, Q., M. Fois, and M. Grisel, *Peel ply surface treatment for composite assemblies: Chemistry and morphology effects.* Composites Part a-Applied Science and Manufacturing, 2005. **36**(11): p. 1562-1568.

[23] Flinn, B.D., et al. *Influence of Peel Ply Type on Adhesive Bonding of Composites Influence of Peel Ply Type on Adhesive Bonding*. in *SAMPE*. 2008.

[24] Palmieri, F.L., et al. *Laser ablation surface preparation of carbon fiber reinforced epoxy composites for adhesive bonding*. in *SAMPE*. 2013.

[25] Singh, R.K., *Identification and Evaluation of Qa Tools for Composite Surface for Adhesive Bonding*. 2015, Cranfield University.

[26] Hart-Smith, L.J., G. Redmond, and M.J. Davis. *The curse of nylon peel ply*. in *41st SAMPE International Symposium and Exhibition*. 1996.



https://dspace.org/

Mechanical performance of composite bonded joints in the presence of localised process-induced zero-thickness defects

Yazdani Nezhad, Hamed; Stratakis, Dimosthenis; Ayre, David; Addepalli, Sri; Zhao, Yifan

2018-11-02
Elsevier
https://doi.org/10.1016/j.promfg.2018.10.175
Hamed Yazdani Nezhad, Dimosthenis Stratakis, David Ayre, et al., Mechanical performance of composite bonded joints in the presence of localised process-induced zero-thickness defects. Procedia Manufacturing, Volume 16, 2018, Pages 91-98

Downloaded from a DSpace repository. https://dspace.org/